996)

ART CLE NO. 0066

Vorticity Boundary Condition and Related Issues for Finite Difference Schemes

WEINAN E* AND JIAN-GUO LIU†

School of Mathematics, Institute for Advanced Study, Princeton, New Jersey 08540

Received May 6, 1994; revised September 11, 1995

This paper discusses three basic issues related to the design of finite difference schemes for *unsteady* viscous incompressible flows using vorticity formulations: the boundary condition for v rticity, an efficient time-stepping procedure, and the relation between these schemes and the ones based on velocity–pressure formulation. We show that many of the newly developed global vorticity boundary conditions can actually be written as some local formulas derived earlier. We also show that if we couple a standard centered difference scheme with third- or fourth-order explicit Runge–Kutta methods, the resulting schemes have *no* cell Reynolds number constraints. For high Reynolds number flows, these schemes are stable under the CFL condition given by the convective terms. Finally, we show that the classical MAC scheme is the same as Thom's formula coupled with second-order centered differences in the interior, in the sense that one can define discrete vorticity in a natural way for the MAC scheme and get the same values as the ones computed from Thom's formula. We use this to derive an efficient fourth-order Runge–Kutta time discretization for the MAC scheme from the one for Thom's formula. We present numerical results for driven cavity flow at high Reynolds number (10^5).

1. INTRODUCTION

In this paper we discuss three basic issues related to the design of finite difference schemes for *unsteady* viscous incompressible flows using vorticity formulation: the boundary condition for vorticity, an efficient time-stepping procedure, and the relation between these schemes and the ones based on velocity–pressure formulation. Our interest will be mainly in the unsteady and possibly turbulent behavior at intermediate time scales, not the ultralong time behavior at low Reynolds number. herefore most of our discussion will not be relevant to steady state calculations. Although throughout this paper we will use mostly forward Euler to illustrate our point, extension to Runge–Kutta schemes is straightforward.

The subject of the vorticity boundary condition in the context of finite difference schemes in vorticity formulation has a long history, going back at least to the 1930s when Thom's formula (see (2.4)) was derived [20]. Thom's formula is generally referred to as being local since vorticity at the boundary is given by a local relation which does not involve coupling to other points at the boundary. There was a resurgence of interest in the 1960s and early 1970s when many variants of Thom's formula were derived (see Section 2 and [18]). But the application of these formulas in actual computations met with only limited success. It was not clear, for example, whether high order formulas such as Pearson's were actually better than lower order ones. Since most of the computations at the time were steady state calculations, these formulas were used in an iterative procedure, and choosing the right relaxation parameter for the iteration was an issue that caused a great deal of confusion. The status as of 1974 was summarized in the review article of Orszag and Israeli [12].

The point of view that has been heavily favored in the last decade is that the vorticity boundary condition has to be global; i.e., one has to solve a system of equations coupling all points on the boundary together to be able to get the boundary value of vorticity. Several ways of obtaining such global vorticity boundary conditions were proposed, most notably the methods of Quartapelle *et al.* [15] and Anderson [1]. A comprehensive review of all these issues can be found in [8].

The main purpose of Section 2 is to show that in the context of finite difference schemes, many of these newly developed global vorticity boundary conditions can actually be written as some local formulas such as Thom's. As examples we will look at Quartapelle's vorticity boundary condition and several versions of Anderson's. We show that the simplest form of Quartapelle's vorticity boundary condition is the same as Thom's formula. The one given by Anderson in [1] is the same as Fromm's formula. We also give a general recipe for converting a discrete form of Anderson's global vorticity boundary condition into local ones. This raises serious doubt on the usefulness of these global boundary conditions since they are much more complicated to implement than the local ones.

* Current address: Courant Institute of Mathematical Sciences, New York University, New York, NY 10012. Email: weinan@cims.nyu.edu.

† On leave from Department of Mathematics, Temple University, Philadelphia, PA 19122. Email: jliu@math.temple.edu.

0021-9991/96 $18.00

Although in Quartapelle's method vorticity at the boundary is given by a local formula in terms of the stream function, the effect is still global since the viscous term must be treated implicitly. Consequently at each time step a coupled system involving vorticity and the stream function has to be solved. Much of the confusion and complexity in this subject comes from solving this coupled system. We will discuss this briefly in Section 2. For more details, we refer the reader to the review articles [12, 8] for early work which resulted in a great deal of confusion and [8, 15] for the more recent treatment which overcomes these earlier problems at the expense of introducing complicated methods. *It is remarkable that all these confusions and complications can be avoided entirely by treating the viscous term explicitly.*

In Section 3 we discuss the issue of the cell Reynolds number constraint in connection with a centered difference scheme. It is well known that for the simple advection equation, centered difference in space and forward Euler in time result in an unconditionally unstable scheme. Although a diffusion term stabilizes the scheme, the cell Reynolds number has to be less than 2 to avoid stability constraints even more severe than the diffusive one. This has often been used as an argument against using centered difference and explicit methods. We show in Section 3 that these problems can be overcome simply by resorting to third- and fourth-order explicit Runge–Kutta methods. This way we avoid all cell Reynolds number constraint caused by stability. For high Reynolds number flows, these schemes are stable under the standard CFL condition given by the convection term. Indeed in the calculations presented in Section 4 and [4] the cell Reynolds number was as high as 10^2 and even 10^3.

In Section 4 we make a few remarks on the relation between the methods discussed here and the MAC type of schemes using primitive variables. We show that Thom's formula coupled with standard second-order centered difference scheme in the vorticity-stream function formulation is the same method as the classical MAC scheme in the sense that there is a natural way to define the discrete vorticity in the MAC scheme, which will have the same values as the ones computed using this centered scheme coupled with Thom's formula in the absence of rounding error. We explore this equivalence between different formulations by translating a straightforward Runge–Kutta method in the vorticity-stream function formulation to an explicit Runge–Kutta procedure for the MAC scheme.

Before ending this introduction let us remark that the main obstacles for designing efficient finite difference methods using the vorticity variable have been the global vorticity boundary condition and the implicit time-stepping, both introduce complicated coupling at the boundary. Once these are cleared, we can design very simple and efficient methods for both 2D and 3D that are high order accurate and have good stability properties. These will be presented in subsequent papers [4, 5].

2. GLOBAL VS LOCAL VORTICITY BOUNDARY CONDITIONS

2.1. *Local Vorticity Boundary Conditions*

The 2D Navier–Stokes equation in vorticity-stream function formulation reads: ($\mathbf{u} = (u, v)$)

$$\begin{aligned} &\partial_t \omega + (\mathbf{u}\cdot\nabla)\omega = \nu\,\Delta\omega,\\ &\Delta\psi = \omega,\\ &u = -\partial_y\phi, \quad v = \partial_x\phi \end{aligned} \tag{2.1}$$

with the boundary condition

$$\psi = 0, \quad \frac{\partial\psi}{\partial\mathbf{n}} = 0.$$

Here we used the no-slip boundary condition. Adding inhomogeneous terms to the boundary condition only amounts to minor changes in what follows. At the grid points, (2.1) is discretized using standard centered difference formulas:

$$\begin{aligned} \frac{d\omega}{dt} - \tilde{D}_y\psi\,\tilde{D}_x\omega + \tilde{D}_x\psi\,\tilde{D}_y\omega = v\,\Delta_h\omega,\\ \Delta_h\psi = \omega, \end{aligned} \tag{2.2}$$

where $\tilde{D}_x$, $\tilde{D}_y$ are the standard centered differences and Δ_h is the standard 5-point Laplacian. We will use i and j to number the grid lines in the x and y directions, respectively, with $i = 0$ at the boundary Γ_y and $j = 0$ at Γ_x. The no penetration boundary condition $\psi = 0$ is imposed on Γ in the solution of the discrete Poisson equation. The no-slip condition is imposed (say on Γ_x) via

$$\frac{\psi_{i,1} - \psi_{i,-1}}{2\,\Delta y} = 0, \tag{2.3}$$

where $(i, -1)$ refers to the "ghost" grid point outside of the computational domain. Since $\psi_{i,0} = \psi_{i-1,0} = \psi_{i+1,0} = 0$, (2.3) implies

$$\begin{aligned} \omega_{i,0} = (\Delta_h\psi)_{i,0} = \frac{\psi_{i+1,0} - 2\psi_{i,0} + \psi_{i-1,0}}{\Delta x^2}\\ + \frac{\psi_{i,1} - 2\psi_{i,0} + \psi_{i,-1}}{\Delta y^2} = \frac{2}{\Delta y^2}\,\psi_{i,1} \end{aligned} \tag{2.4}$$

which is the well-known Thom's formula.

TABLE I

Summary of Variants of Thom's Formula

Reference	$\omega - \psi$ formulation	MAC scheme
Thom, 1933	$\omega_{0,j} = \frac{2}{\Delta x^2}\psi_{1,j}$ $\psi_{-1,j} = \psi_{1,j}$	$v_{-1/2,j} = -v_{1/2,j}$
Woods, 1954	$\omega_{0,j} = \frac{3}{\Delta x^2}\psi_{1,j} - \frac{1}{2}\omega_{1,j}$	$v_{-1/2,j} = -\frac{5}{2}v_{1/2,j} + \frac{1}{2}v_{3/2,j} - \frac{1}{2\Delta y}(u_{1,j+1/2} - u_{1,j-1/2})$
Fromm, 1963	$\omega_{0,j} = \frac{1}{\Delta x^2}\psi_{1,j}$ $\psi_{-1,j} = 0$	$v_{-1/2,j} = 0$
Wilkes, 1963	$\omega_{0,j} = \frac{1}{2\Delta x^2}(8\psi_{1,j} - \psi_{2,j})$	$v_{-1/2,j} = -\frac{5}{2}v_{1/2,j} + \frac{1}{2}v_{3/2,j}$
Pearson, 1965	$\psi_{-1,j} = 3\psi_{1,j} - \frac{1}{2}\psi_{2,j}$	
Orszag and Israeli, 1974	$\omega_{0,j} = \frac{1}{3\Delta x^2}(10\psi_{1,j} - \psi_{2,j})$ $\psi_{-1,j} = \frac{7}{3}\psi_{1,j} - \frac{1}{3}\psi_{2,j}$	$v_{-1/2,j} = -2v_{1/2,j} + \frac{1}{3}v_{3/2,j}$
Orszag and Israeli, 1974	$\omega_{0,j} = \frac{1}{13\Delta x^2}(35\psi_{1,j} - \psi_{3,j})$ $\psi_{-1,j} = \frac{22}{13}\psi_{1,j} - \frac{1}{13}\psi_{3,j}$	$v_{-1/2,j} = -\frac{21}{13}v_{1/2,j} + \frac{1}{13}v_{3/2,j} + \frac{1}{13}v_{5/2,j}$

Many variants of Thom's formulas have been proposed. For later reference we summarize them here in Table I. In the spirit of Section 4, we will list the equivalent formulas in the velocity variable when the MAC scheme is used in the interior. To understand how these formulas were derived, we also provide the interpretation of these formulas in terms of the boundary condition $\partial\psi/\partial\mathbf{n} = 0$. The vorticity boundary conditions are obtained from the Neumann boundary condition for ψ, together with the second-order formula: $\omega_{0,j} = (\Delta_h\psi)_{0,j}$. Woods' formula appears special in this table since it involves interior values of vorticity.

High order formulas can also be found in the literature. For example, a fourth-order accurate formula can be obtained by using the one-sided difference approximation for the Neumann boundary condition for ψ,

$$\psi_{-1,j} = 6\psi_{1,j} - 2\psi_{2,j} + \tfrac{1}{3}\psi_{3,j},$$

together with the one-sided formula

$$\begin{aligned}\omega_{0,j} &= (\partial_x^2\psi)_{0,j}\\ &= \frac{1}{12\Delta x^2}(11\psi_{-1,j} + 6\psi_{1,j} + 4\psi_{2,j} - \psi_{3,j}) + O(h^4).\end{aligned}$$

The combination gives

$$\omega_{0,j} = \frac{1}{18\Delta x^2}(108\psi_{1,j} - 27\psi_{2,j} + 4\psi_{3,j}),$$

This formula was derived in Briley [2].

We implemented these formulas for the unsteady Stokes equation on the domain $[-1, 1] \times [0, 2\pi]$ with no-slip boundary condition in the x-direction and periodic boundary condition in the y-direction. An exact solution of this problem is given by [13]:

$$u(x, y, t) = \hat{u}(x)e^{iy+\sigma t}, \quad v(x, y, t) = \hat{v}(x)e^{iy+\sigma t},$$
$$p(x, y, t) = \hat{p}(x)e^{iy+\sigma t},$$

where

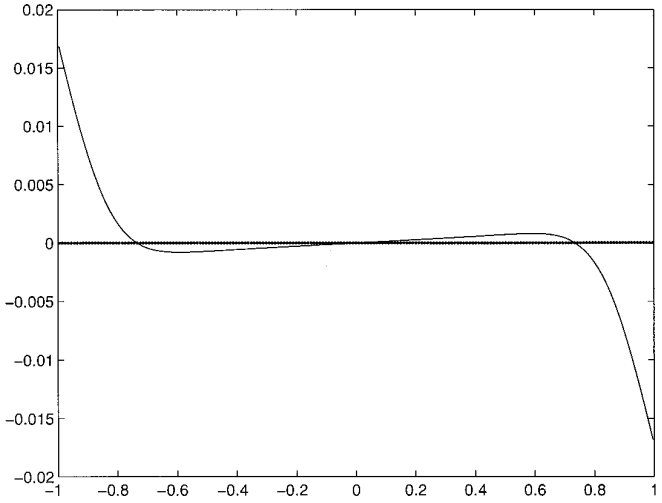

FIG. 1. Relative error in v for the Fromm's formula (solid line), Thom's formula (dashed line), Wilkes–Pearson's formula (dotted line), and Orszag–Israeli's formula (dot-dashed line). Time is discretized using mid-point rule. The errors for Thom's formula, Wilkes–Pearson's formula, and Orszag–Israeli's formula are too small to be seen on this graph. Parameters: viscosity = 0.01, $\Delta t = 0.001$, $\Delta x = 0.01$.

$$\hat{u}(x) = \cos \mu x - \cos \mu \frac{\cosh x}{\cosh 1},$$

$$\hat{v}(x) = \frac{\mu}{i} \sin \mu x + \frac{1}{i} \cos \mu \frac{\sinh x}{\cosh 1},$$

$$\hat{p}(x) = \sigma \cos \mu \frac{\sinh x}{\cosh 1},$$

$\mu = 2.8833556585893$, $\sigma = -\nu(\mu^2 + 1)$. The time step was chosen to be sufficiently small so that the error in time discretization is negligible. The relative error for v at time $t = 1$ with $\nu = 0.01$, $\Delta x = 0.01$ is given in Figs. 1 and 2 for Fromm's, Thom's, Wilkes–Pearson's, and Orszag and Israeli's (the first of the two) formulas. As expected, Fromm's formula performs poorly since it is only first-order accurate. The other three give more or less comparable results. Orszag and Israeli's formula does slightly better at the boundary.

2.2. *Quartapelle's Vorticity Boundary Condition*

In the spatially continuous form we can state the constraint on vorticity as follows: ω is such that the overdetermined problem

$$\begin{aligned} \Delta \psi &= \omega, \\ \psi|_\Gamma = 0, \quad & \left.\frac{\partial \psi}{\partial \mathbf{n}}\right|_\Gamma = 0, \end{aligned} \tag{2.5}$$

has a solution. The key idea, due to Quartapelle and Valz-Gris [16], is the following: (2.5) has a solution if and only if ω is orthogonal (with respect to the standard L^2 inner product) to $\mathcal{H}$, the space of harmonic functions on Ω.

Quartapelle and co-workers have suggested several ways of implementing this idea, with the viscous term treated implicitly. One attractive feature of this formulation is the flexibility of spatial discretization: finite difference, finite element, and spectral methods can all be used. In the context of finite difference schemes, the simplest implementation of Quartapelle's method amounts to the following:

$$\begin{aligned} \frac{\omega^{n+1} - \omega^n}{\Delta t} + (\mathbf{u}^n \cdot \nabla_h)\omega^n &= \nu \Delta_h \omega^{n+1} \quad \text{for } i, j \geq 1, \\ \Delta_h \psi^{n+1} &= \omega^{n+1} \quad \text{for } i, j \geq 1, \\ \psi^{n+1}|_\Gamma &= 0, \\ D_{\mathbf{n}} \psi^{n+1}|_\Gamma &= 0. \end{aligned} \tag{2.6}$$

($D_{\mathbf{n}}$ is a finite difference approximation to $\partial/\partial \mathbf{n}$.) The key here is that at the time step $n + 1$, both boundary conditions on ψ^{n+1} are satisfied. Quartapelle *et al.* suggested the following procedure to implement this [15]:

Step 1. Form a system of the form

$$A \omega_{\mathrm{b}}^{n+1} = \beta \tag{2.7}$$

for the boundary values of vorticity at the new time step by requiring that ω^{n+1} be orthogonal to all the discrete harmonic functions.

Step 2. Solve (2.7) to obtain the boundary value of ω^{n+1}, $\omega_{\mathrm{b}}^{n+1}$.

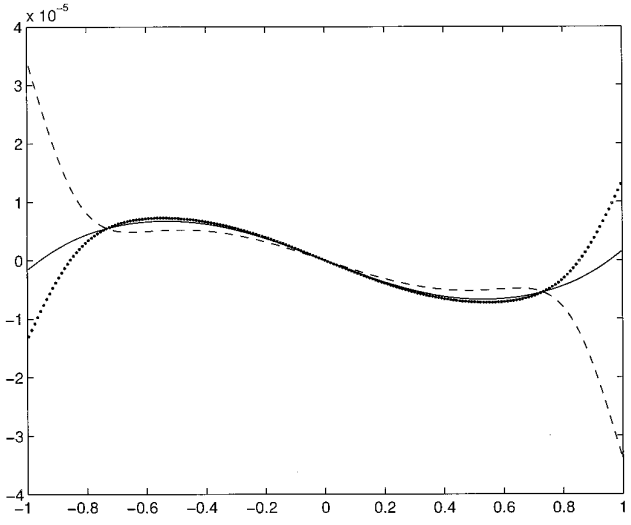

FIG. 2. Relative error in v for the Thom's formula (dashed line), Wilkes–Pearson's formula (dotted line), and Orszag–Israeli's formula (solid line). Parameters: viscosity = 0.01, $\Delta t = 0.001$, $\Delta x = 0.01$.

Step 3. Solve the first equation in (2.6) to get ω^{n+1}.

This method requires knowing all the discrete harmonic functions and/or discrete Green's function at all boundary points. These are linear spaces with dimension N equal to the number of grid points at the boundary. This might not be too bad for 2D but it is prohibitively expensive for 3D. Knowing all the discrete harmonic functions, one can construct the matrix A (which is a full matrix) at the preprocessing stage. Then forming (2.7) at each time step only requires the computation of β. This is still quite expensive, though, since it requires the evaluation of N volume integrals. For the details see [15].

If $D_{\mathbf{n}}$ is approximated by the centered difference, then it follows from the derivation presented in the beginning of this section that

$$\omega_{i,0}^{n+1} = \frac{2}{\Delta y^2}\psi_{i,1}^{n+1}, \quad \omega_{0,j}^{n+1} = \frac{2}{\Delta x^2}\psi_{1,j}^{n+1}, \quad i,j \geq 0. \tag{2.8}$$

which is the same as Thom's formula.

If, on the other hand, $D_{\mathbf{n}}$ is approximated by first-order one-sided difference, i.e.,

$$(D_{\mathbf{n}}\psi)_{i,0} = \frac{\psi_{i,1} - \psi_{i,0}}{\Delta y} \quad \text{on } \Gamma_x, \tag{2.9}$$

then a similar derivation gives

$$\omega_{i,0}^{n+1} = \frac{1}{\Delta y^2}\psi_{i,1}^{n+1}, \quad \omega_{0,j}^{n+1} = \frac{1}{\Delta x^2}\psi_{1,j}^{n+1}, \quad i,j \geq 0, \tag{2.10}$$

which is Fromm's formula.

Remark. Although (2.8) and (2.10) seem local, they are not truly local since ψ^{n+1} is affected by ω^{n+1} everywhere, due to the implicit treatment of the viscous term. Since ψ^{n+1} and ω^{n+1} are coupled together by the boundary condition, a coupled system (2.6) has to be solved at each time step. This is where difficulties arise.

The old approach, widely used in the 1960s, is to solve (2.6) using an iterative procedure. A simple example is the following: Set $\omega^{n+1,0} = \omega^n$ and for $m = 0, 1, 2, \ldots$ use

$$\begin{aligned}
&\frac{\omega^{n+1,m+1} - \omega^n}{\Delta t} - \tilde{D}_y\psi^n\,\tilde{D}_x\omega^n \\
&\quad + \tilde{D}_x\psi^n\,\tilde{D}_y\omega^n = \nu\,\Delta_h\omega^{n+1,m}, \\
&\Delta_h\psi^{n+1,m+1} = \omega^{n+1,m+1}, \\
&\psi^{n+1,m+1}|_\Gamma = 0, \\
&\omega_{i,0}^{n+1,m+1} = \frac{2}{\Delta y^2}\psi_{i,1}^{n+1,m+1}, \\
&\omega_{0,j}^{n+1,m+1} = \frac{2}{\Delta x^2}\psi_{1,j}^{n+1,m+1},
\end{aligned} \tag{2.11}$$

until convergence is reached. As it turns out, this is not such a good method for solving the coupled system (2.6). It may even diverge [12] and some kind of relaxation is necessary to get convergence. Furthermore, it appears that for higher order formulas such as Pearson's, convergence is more difficult to reach. This is the main reason for the difficulties described in [12].

In the last decade or so, new approaches such as the influence matrix techniques are developed to solve (2.6). Typically a key step in these new methods is to form and solve (2.7) for the boundary value of vorticity. While overcoming the difficulties mentioned earlier, these new methods are troubled by their complexity, overhead, and storage requirement. We refer to [8, 15] for details of these new methods.

In contrast, if we had treated the viscous term *explicitly,* i.e., replacing (2.6) by

$$\begin{aligned}
&\frac{\omega^{n+1} - \omega^n}{\Delta t} + (\mathbf{u}^n \cdot \nabla_h)\omega^n = \nu\,\Delta_h\omega^n \quad \text{for } i,j \geq 1, \\
&\Delta_h\psi^{n+1} = \omega^{n+1} \quad \text{for } i,j \geq 1, \\
&\psi^{n+1}|_\Gamma = 0, \\
&D_{\mathbf{n}}\psi^{n+1}|_\Gamma = 0,
\end{aligned} \tag{2.12}$$

then the resulting scheme can be realized by a simple three-step marching procedure. Given $\{\omega_{i,j}^n\}, \{\omega_{i,j}^{n+1}\}$ is computed by:

Step 1. Update the vorticity at the interior grid points by

$$\frac{\omega^{n+1} - \omega^n}{\Delta t} - \tilde{D}_y\psi^n\,\tilde{D}_x\omega^n + \tilde{D}_x\psi^n\,\tilde{D}_y\omega^n = \nu\,\Delta_h\omega^n. \tag{2.13}$$

Step 2. Solve

$$\Delta_h\psi^{n+1} = \omega^{n+1}, \tag{2.14}$$

with the boundary condition $\psi^{n+1}|_\Gamma = 0$.

Step 3. Update the vorticity at the boundary using

$$\omega_{i,0}^{n+1} = \frac{2}{\Delta y^2}\psi_{i,1}^{n+1}, \quad \omega_{0,j}^{n+1} = \frac{2}{\Delta x^2}\psi_{1,j}^{n+1}. \tag{2.15}$$

It is important that (2.14) can be solved without knowing the boundary value of ω^{n+1}. Hence *there is no need to iterate between ψ^{n+1} and the boundary value of ω^{n+1}.* At every time step, only one *standard* Poisson solve is required.

2.3. *Anderson's Vorticity Boundary Condition*

At the continuous level, Anderson's method can be formulated as follows: If $D_{\mathbf{n}}\psi|_\Gamma = 0$ at $t = 0$, then $D_{\mathbf{n}}\psi|_\Gamma = 0$ is equivalent to $D_{\mathbf{n}}(\partial\psi/\partial t)|_\Gamma = 0$. Since

$$\frac{\partial\psi}{\partial t} = \Delta_0^{-1}\frac{\partial\omega}{\partial t} = \Delta_0^{-1}(-(\mathbf{u}\cdot\nabla)\omega + \nu\,\Delta\omega)$$

(the subscript 0 means the homogeneous Dirichlet boundary condition is taken), we can write the boundary condition $D_{\mathbf{n}}\psi|_\Gamma = 0$ as

$$D_{\mathbf{n}}\Delta_0^{-1}(-(\mathbf{u}\cdot\nabla)\omega + \nu\,\Delta\omega) = 0. \tag{2.16}$$

When a spatial discretization is taken, this becomes

$$D_{\mathbf{n}}\Delta_{h,0}^{-1}(-(\mathbf{u}\cdot\nabla_h)\omega + \nu\,\Delta_h\omega) = 0. \tag{2.17}$$

Writing $\omega = \omega_{\text{in}} + \omega_{\text{bd}}$, where ω_{bd} vanishes at the interior grid points and ω_{in} vanishes at boundary grid points, we get

$$\begin{aligned} &D_{\mathbf{n}}\Delta_{h,0}^{-1}(-(\mathbf{u}\cdot\nabla_h)\omega_{\text{bd}} + \nu\,\Delta_h\omega_{\text{bd}}) \\ &\quad = -D_{\mathbf{n}}\Delta_{h,0}^{-1}(-(\mathbf{u}\cdot\nabla_h)\omega_{\text{in}} + \nu\,\Delta_h\omega_{\text{in}}). \end{aligned} \tag{2.18}$$

This is Anderson's formulation of the vorticity boundary condition.

In the following, we present several examples of implementing (2.18) in a fully discrete scheme and show that in all these cases, (2.18) can be written as local formulas.

The first example is the original Anderson's method presented in [1]. Here Δ_h is the standard 5-point Laplacian. Let $\Delta_{h,0}\omega$ be the discrete Laplacian of ω using zero as the boundary value of ω. Given $\{\omega_{i,j}^n\}_{i,j\geq 1}$, Anderson's method for computing $\{\omega_{i,j}^{n+1}\}_{i,j\geq 1}$ consists of the following three steps [1]. The purpose of the first and second steps is to compute the boundary value of ω^n, ω_b^n.

Step 1. Solve $\Delta_{h,0}\psi^n = \omega^n$, compute $\mathbf{u}^n = (-\tilde{D}_y\psi^n, \tilde{D}_x\psi^n)$ at the interior mesh points, and then compute $\tilde{F} = (\mathbf{u}^n\cdot\nabla_h)\omega^n - \nu\,\Delta_{h,0}\omega^n$ at the interior mesh points. At the boundary the nonlinear convective term is computed using the one-sided difference. Therefore this step does not involve the boundary value of ω^n.

Step 2. Determine the boundary value of ω^n by solving

$$D_{\mathbf{n}}\Delta_{h,0}^{-1}(\nu\,\Delta_h\omega_b^n) = D_{\mathbf{n}}\,\Delta_{h,0}^{-1}\tilde{F}. \tag{2.19}$$

Here ω_b^n is identified as it has been extended to all the interior mesh points with the value zero; $D_{\mathbf{n}}$ is a finite difference approximation of $\partial/\partial\mathbf{n}$ on Γ. In [1], Anderson chose the first-order one-sided formula (2.9).

Step 3. Compute

$$\omega^{n+1} = \omega^n + \Delta t(-(\mathbf{u}^n\cdot\nabla_h)\omega^n + \nu\,\Delta_h\omega^n) \tag{2.20}$$

at all the interior mesh points, where the boundary value of ω^n is taken as ω_b^n.

The effect of Steps 1 and 2 is to ensure that

$$D_{\mathbf{n}}\psi^{n+1} = 0, \quad \psi^{n+1} = \Delta_{h,0}^{-1}\omega^{n+1} \tag{2.21}$$

when ω^{n+1} is computed from (2.20). In particular, we have $\psi^{n+1} = 0$ not only on Γ but also at the grid points next to Γ. We can write Anderson's method as

$$\begin{aligned} &\frac{\omega^{n+1}-\omega^n}{\Delta t} + (\mathbf{u}^n\cdot\nabla)\omega^n = \nu\,\Delta_h\omega^n \\ &\qquad\qquad \text{at interior grid points,} \\ &\Delta_{h,0}\psi^{n+1} = \omega^{n+1}, \\ &D_{\mathbf{n}}\psi^{n+1} = 0 \quad \text{at } \Gamma_x, \Gamma_y. \end{aligned} \tag{2.22}$$

Anderson's three-step formulation can be stated as: Given $\{\omega_{i,j}^n\}_{i,j\geq 1}$, there exists a unique $\omega_b^n = \omega^n|_\Gamma$, namely the solution of (2.19), such that (2.22) has a unique set of solutions $\{\omega_{i,j}^{n+1}\}_{i,j\geq 1}$, $\{\psi_{i,j}^{n+1}\}_{i,j\geq 0}$. Notice that ω_b^n is just an auxiliary variable used to obtain $\{\omega_{i,j}^{n+1}\}_{i,j\geq 1}$, $\{\psi_{i,j}^{n+1}\}_{i,j\geq 0}$.

There is a much simpler way of implementing (2.22), without even thinking about $\omega_b^n = \omega^n|_\Gamma$. In this formulation, it is helpful to think of the lines $\Gamma_h' = \{i = 1\}\cup\{j = 1\}$ as the numerical boundary, even though the method is exactly the same as (2.22).

Initialization. Given $\{\omega_{i,j}^0\}_{i,j\geq 1}$, define $\psi^0|_\Gamma = 0$ and solve

$$\begin{aligned} &\Delta_h\psi^0 = \omega^0, \quad i,j \geq 2, \\ &\psi^0|_{\Gamma_h'} = 0. \end{aligned}$$

Modify $\omega^0|_{\Gamma_h'}$ such that

$$\omega_{i,1}^0 = \frac{1}{\Delta y^2}\,\psi_{i,2}^0, \quad \omega_{1,j}^0 = \frac{1}{\Delta x^2}\,\psi_{2,j}^0.$$

This is to ensure that ψ^0 is a solution of

$$\begin{aligned} &\Delta_h\psi^0 = \omega^0, \quad i,j \geq 1, \\ &\psi^0|_\Gamma = 0. \end{aligned} \tag{2.23}$$

In other words, the solution of (2.23) actually satisfies $\psi^0|_{\Gamma_h'} = 0$, i.e., $D_{\mathbf{n}}\psi^0|_\Gamma = 0$.

Time-stepping procedure. Given $\{\omega_{i,j}^n\}_{i,j\geq 1}$, such that $\psi^n = \Delta_{h,0}^{-1}\omega^n$ also satisfies $D_n\psi^n|_\Gamma = 0$, i.e., $\psi^n|_{\Gamma_h'} = 0$.

Step 1. Compute

$$\frac{\omega^{n+1}-\omega^n}{\Delta t}+(\mathbf{u}^n\cdot\nabla)\omega^n=\nu\Delta_h\omega^n \quad \text{for } i,j\geq 2. \tag{2.24}$$

Step 2. Let $\psi^{n+1}|_\Gamma=0$ and solve

$$\begin{aligned}\Delta_h\psi^{n+1}&=\omega^{n+1}, \quad i,j\geq 2,\\ \psi^{n+1}|_{\Gamma_h'}&=0,\end{aligned}$$

and set

$$\omega_{i,1}^{n+1}=\frac{1}{\Delta y^2}\psi_{i,2}^{n+1}, \quad \omega_{1,j}^{n+1}=\frac{1}{\Delta x^2}\psi_{2,j}^{n+1}, \quad i,j\geq 1,$$

which is Fromm's formula. This last step has the effect of ensuring that ψ^{n+1} is also a solution of

$$\begin{aligned}\Delta_h\psi^{n+1}&=\omega^{n+1}, \quad i,j\geq 1,\\ \psi^{n+1}|_\Gamma&=0,\end{aligned}$$

i.e., $\psi^{n+1}=\Delta_{h,0}^{-1}\omega^{n+1}$ satisfies both the Dirichlet and Neumann boundary conditions:

$$\psi^{n+1}|_\Gamma=0, \quad D_{\mathbf{n}}\psi^{n+1}|_\Gamma=0.$$

The Neumann boundary condition is the same as $\psi^{n+1}|_{\Gamma_h'}=0$.

It is obvious that the numerical solutions obtained through this procedure satisfy (2.22). Therefore this is exactly the same method as Anderson's. The global vorticity boundary condition (2.19) is replaced by Fromm's formula. In other words, *the effect of implementing Anderson's global boundary condition on* Γ *is exactly the same as implementing Fromm's formula on* Γ_h'. To make the connection more transparent, let us remark that after obtaining $\{\omega_{i,j}^{n+1}\}_{i,j\geq 1}$, one can find ω_b^n by requiring that (2.19) also hold for i or $j=1$, i.e., on Γ_h'. This gives the solution of ω_b^n. However, it is important to realize that the method can be implemented without using ω_b^n.

In the method discussed above, it is straightforward to replace the forward Euler by the higher order explicit Runge–Kutta and require that the no-slip boundary condition be satisfied at each stage of the Runge–Kutta method. A second-order time discretization was presented in [17]. The same argument as we presented above can then be applied to each stage, proving that in this case Anderson's vorticity boundary condition is still the same as Fromm's formula.

If we replace the first-order accurate formula (2.9) by a second-order one-sided difference:

$$(\overline{D}_{\mathbf{n}}\psi)_{i,0}=\frac{4\psi_{i,1}-\psi_{i,2}-3\psi_{i,0}}{2\,\Delta y}, \tag{2.25}$$

we can still write Anderson's method as (2.22) with $D_{\mathbf{n}}$ replaced by $\overline{D}_{\mathbf{n}}$. To understand the connection with local formulas in this case we break

$$\begin{aligned}\Delta_{h,0}\psi^{n+1}&=\omega^{n+1},\\ \overline{D}_{\mathbf{n}}\psi^{n+1}&=0 \quad \text{at } \Gamma_x,\Gamma_y\end{aligned} \tag{2.26}$$

into several pieces:

1. Set $\psi_{i,0}^{n+1}=0$, $\psi_{0,j}^{n+1}=0$, $i,j\geq 0$.
2. Solve

$$\begin{aligned}\Delta_h\psi^{n+1}&=\omega^{n+1},\\ \frac{4\psi_{i,1}^{n+1}-\psi_{i,2}^{n+1}}{2\,\Delta y}&=0, \quad \frac{4\psi_{1,j}^{n+1}-\psi_{2,j}^{n+1}}{2\,\Delta x}=0\end{aligned} \tag{2.27}$$

for $\{\psi_{i,j}^{n+1}\}_{i,j\geq 1}$.

3. Compute

$$\omega_{i,1}^{n+1}=(\Delta_h\psi^{n+1})_{i,1}, \quad \omega_{1,j}^{n+1}=(\Delta_h\psi^{n+1})_{1,j}. \tag{2.28}$$

As before, this is just a different way of implementing (2.26). Using (2.27) and (2.28), we get

$$\begin{aligned}\omega_{i,1}^{n+1}=(\Delta_h\psi^{n+1})_{i,1}&=\frac{1}{h^2}(\psi_{i,2}^{n+1}+\psi_{i+1,1}^{n+1}+\psi_{i-1,1}^{n+1}-4\psi_{i,1}^{n+1})\\ &=\frac{1}{4h^2}(\psi_{i+1,2}^{n+1}+\psi_{i-1,2}^{n+1})\\ &=\frac{1}{4}\omega_{i,2}^{n+1}+\frac{15}{16h^2}\psi_{i,2}^{n+1}-\frac{1}{4h^2}\psi_{i,3}^{n+1}.\end{aligned} \tag{2.29}$$

This can be viewed as

$$\omega_{i,0}=\frac{1}{4}\omega_{i,1}+\frac{15}{16h^2}\psi_{i,1}-\frac{1}{4h^2}\psi_{i,2} \tag{2.30}$$

imposed on Γ'. Equation (2.30) is analogous to Woods' formula but is slightly more complicated.

This can be formulated as a general recipe for converting Anderson's vorticity boundary condition into local formulas. To explain this, let us take the example of a fourth-order spatial discretization in which $\partial^2/\partial x^2$ is approximated by the standard five-point fourth-order formula $D_x^2(1-(h^2/12)D_x^2)$, and the boundary condition $D_{\mathbf{n}}\psi|_\Gamma=0$ is used twice at the boundary with one-sided fourth-order approximation for $D_{\mathbf{n}}$. In [17], a fourth-order implementation of Anderson's method was outlined but no details were given.

The above strategy is the closest we can think of to fit the outline. Again we will use forward Euler as an illustration since extension to the high order explicit Runge–Kutta is straightforward.

Because of the wide stencil used, vorticity boundary conditions are needed at the two rows of grid points near the boundary. Written in terms of $\omega = \omega_{\text{in}} + \omega_{\text{bd}}$, Anderson's vorticity boundary conditions are

$$\overline{D}_{\mathbf{n}}(\tilde{\Delta}_{h,0}^{-1}\omega^{n+1}) = 0, \quad \tilde{D}_{\mathbf{n}}(\tilde{\Delta}_{h,0}^{-1}\omega^{n+1}) = 0, \tag{2.31}$$

where $\overline{D}_{\mathbf{n}}$ and $\tilde{D}_{\mathbf{n}}$ are two one-sided (fourth-order) approximations to $D_{\mathbf{n}}$, $\tilde{\Delta}_h = D_x^2(1 - (h^2/12)D_x^2) + D_y^2(1 - (h^2/12)D_y^2)$, except at i, or $j = 1$, where it has to be modified to make it slightly one-sided. To obtain the equivalent local formulas, we can proceed as follows. For concreteness we concentrate on Γ_x:

We split (2.31) into several pieces:

(1) Set $\psi_{i,0}^{n+1} \equiv 0$.

(2) Solve

$$\tilde{\Delta}_h\psi^{n+1} = \omega^{n+1} \quad \text{for } i \geq 3,$$

using $\tilde{D}_{\mathbf{n}}\psi^{n+1}|_\Gamma = 0$, $\overline{D}_{\mathbf{n}}\psi^{n+1}|_\Gamma = 0$ as boundary conditions for $\{\psi_{i,1}^{n+1}, \psi_{i,2}^{n+1}\}$.

(3) Define

$$\omega_{i,1}^{n+1} = (\tilde{\Delta}_h\psi^{n+1})_{i,1}, \quad \omega_{i,2}^{n+1} = (\tilde{\Delta}_h\psi^{n+1})_{i,2}. \tag{2.32}$$

(1)–(3) is equivalent to

$$\tilde{\Delta}_{h,0}\psi^{n+1} = \omega^{n+1}$$
$$\overline{D}_{\mathbf{n}}\psi^{n+1}|_\Gamma = 0, \quad \tilde{D}_{\mathbf{n}}\psi^{n+1}|_\Gamma = 0,$$

which is the same as (2.31).

Equations (2.32) are the local formula we are looking for. This seems to be far more complicated than Briley's formula mentioned earlier which is also fourth-order accurate.

3. CELL REYNOLDS NUMBER CONSTRAINT AND HIGH ORDER RUNGE–KUTTA METHODS

It is well known that if we use second-order centered difference in space and forward Euler in time for the simple advection equation,

$$u_t + au_x = 0, \tag{3.1}$$

the resulting scheme is unconditionally unstable. This has the consequence that for the advection-diffusion equation,

$$u_t + au_x = \nu u_{xx}, \tag{3.2}$$

this scheme is stable only under the constraint

$$\Delta t\left(\frac{a^2}{2\nu} + \frac{2\nu}{\Delta x^2}\right) < 1. \tag{3.3}$$

Therefore, we must have

$$\nu\frac{\Delta t}{\Delta x^2} < \frac{1}{2}, \quad \Delta t < \frac{2\nu}{a^2}. \tag{3.4}$$

The first condition in (3.4) is the standard diffusive constraint on time steps. The second one reflects the fact that the scheme is unstable if $\nu = 0$.

We can rewrite this second condition as

$$\frac{a\,\Delta t}{L} < \frac{2}{\text{Re}}, \tag{3.5}$$

where L is the size of the computational domain and $\text{Re} = La/\nu$ is the Reynolds number. The spatial resolution should be chosen to resolve the smallest active scale in the flow. This means that at high Reynolds number we should take $\Delta x/L = O(\text{Re}^{-1/2})$ for 2D, and $\Delta x/L = O(\text{Re}^{-3/4})$ for 3D. Consequently we have from (3.5)

$$\frac{a\,\Delta t}{\Delta x} < O(\text{Re}^{-1/2}), \quad \frac{a\,\Delta t}{\Delta x} < O(\text{Re}^{-1/4}) \tag{3.6}$$

for 2D and 3D, respectively. This is a severe constraint, since ideally we want $a\,\Delta t/\Delta x = O(1)$ for $\text{Re} \gg 1$.

From a slightly different point of view, if we demand the second condition in (3.4) to be less restrictive than the standard diffusive condition, we should take

$$\frac{2\nu}{a^2} > \frac{\Delta x^2}{2\nu}, \quad \text{i.e., } \text{Rc} = \frac{a\,\Delta x}{\nu} < 2; \tag{3.7}$$

Rc is called the cell Reynolds number. Inequality (3.3) and this stability-caused cell Reynolds number constraint has often been used as an argument against using centered differencing for the convection term at high Reynolds number.

It is important to realize that these constraints still remain even if we discretize the diffusion term implicitly, keeping the advection term explicit. Since the problem comes from the advection term, at high Reynolds number the diffusion term is of very little help. Although such constraints do disappear if we discretize the advection term also implicitly, this is far too expensive. As we show below, there is a much simpler solution to this problem.

What causes this instability and the subsequent cell Reynolds number constraint is the fact that the stability region of the forward Euler method does not contain any part of the imaginary axis. The same is true for the second-order explicit Runge–Kutta methods, but not for third- and fourth-order ones. The Fourier symbol for the centered difference operator $-a\tilde{D}_x + \nu D_x^2$ is $C(\xi) = ia \sin(\xi/\Delta x) - (4\nu/\Delta x^2) \sin^2(\xi/2)$. Therefore if we use the fourth-order Runge–Kutta in time, the two stability conditions are

$$\frac{a\,\Delta t}{\Delta x} \le C_1, \quad 4\nu \frac{\Delta t}{\Delta x^2} \le C_2, \tag{3.8}$$

where C_1 and C_2 are some constants (for example, they can be taken as 1.5). There is no cell Reynolds number constraint imposed by stability considerations. The same conclusions can be drawn for the third-order Runge–Kutta method. From the point of view of accuracy, for $\mathrm{Re} \gg 1$, $\mathrm{Rc} = \mathrm{Re}(\Delta x/L) = O(\mathrm{Re}^{1/2})$ for 2D and $O(\mathrm{Re}^{1/4})$ for 3D. This does not present a constraint on the cell Reynolds number either. Indeed in the calculations presented in Section 4 and [4], the cell Reynolds number is as high as 10^2 and even 10^3. In particular, for $\mathrm{Rc} = a\,\Delta x/\nu > C_1/4C_2$, the size of Δt is controlled only by the CFL condition coming from the convection terms.

4. MAC SCHEME AND THOM'S FORMULA

4.1. *MAC Scheme*

The MAC scheme [14] uses the velocity–pressure formulation of the incompressible Navier–Stokes equation,

$$\begin{aligned} \partial_t \mathbf{u} + (\mathbf{u}\cdot\nabla)\mathbf{u} + \nabla p &= \nu\,\Delta\mathbf{u}, \\ \nabla\cdot\mathbf{u} &= 0, \end{aligned} \tag{4.1}$$

where $\mathbf{u} = (u, v)$. A special feature of the MAC scheme is the use of the staggered grid (Fig. 3). One such grid is displayed in Fig. 3, where the pressure variable p is defined at "□" points, the first and second component of the velocity u and v are defined at "△" and "○" points, respectively. Define

$$\tilde{D}_x u(x,y) = \frac{u(x+\Delta x, y) - u(x-\Delta x, y)}{2\,\Delta x},$$

$$D_x u(x,y) = \frac{u(x+\Delta x/2, y) - u(x-\Delta x/2, y)}{\Delta x},$$

$$\tilde{E}_x u(x,y) = \frac{u(x+\Delta x, y) + u(x-\Delta x, y)}{2},$$

$$E_x u(x,y) = \frac{u(x+\Delta x/2, y) + u(x-\Delta x/2, y)}{2},$$

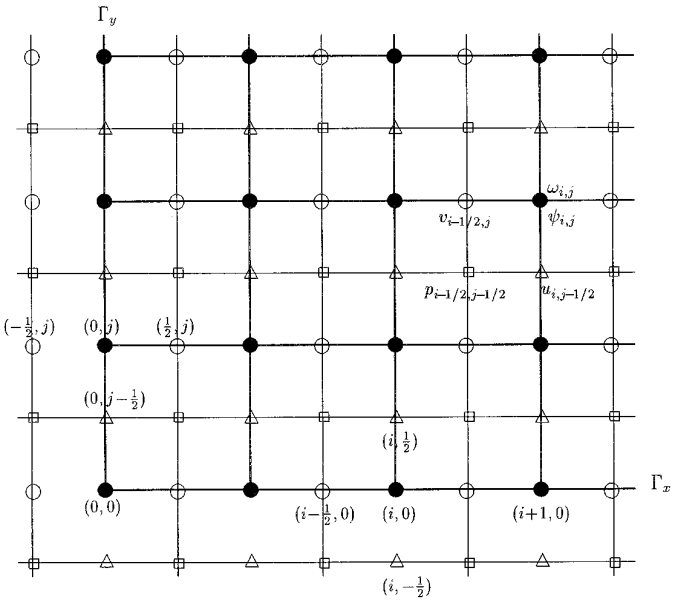

FIG. 3. Staggered grid in the interior and at the boundary.

and similarly for $\tilde{D}_y u$, $\tilde{E}_y u$, $D_y u$, $E_y u$; and

$$\Delta_h u = (D_x^2 + D_y^2)u,$$

we can write the MAC scheme as

$$\begin{aligned} &\frac{du}{dt} + u\,\tilde{D}_x u + E_x E_y v\,\tilde{D}_y u + D_x p = \nu\,\Delta_h u, && \text{at "△" points,} \\ &\frac{dv}{dt} + E_x E_y u\,\tilde{D}_x v + v\,\tilde{D}_y v + D_y p = \nu\,\Delta_h v, && \text{at "○" points,} \\ &D_x u + D_y v = 0, && \text{at "□" points.} \end{aligned} \tag{4.2}$$

The simplest way of treating the boundary is to use the reflection technique. On the segment Γ_x (see Fig. 3), the boundary condition $v = 0$ is imposed exactly at the "○" points: $v_{i-1/2,0} = 0$; the boundary condition $u = 0$ is imposed approximately at the "●" points by letting

$$u_{i,-1/2} = -u_{i,1/2}. \tag{4.3}$$

Similarly on Γ_y, we have

$$v_{-1/2,j} = -v_{1/2,j}, \quad u_{0,j-1/2} = 0.$$

Some doubts on the consistency of the reflection technique near the boundary were expressed in [14]. We show in Appendix 2 that while a naive truncation error analysis does seem to suggest that (4.3) leads to inconsistency near

the boundary, a more careful analysis shows that there is still overall second-order accuracy, even at the boundary.

The fully discrete MAC scheme, with the viscous term treated explicitly, is given by

$$\begin{aligned}
&\frac{u^{n+1}-u^n}{\Delta t} + u^n \tilde{D}_x u^n + E_x E_y v^n \tilde{D}_y u^n \\
&\quad + D_x p^n = \nu \Delta_h u^n, \\
&\quad \text{at ``}\Delta\text{'' points,} \\
&\frac{v^{n+1}-v^n}{\Delta t} + E_x E_y u^n \tilde{D}_x v^n + v^n \tilde{D}_y v^n \\
&\quad + D_y p^n = \nu \Delta_h v^n, \\
&\quad \text{at ``}\bigcirc\text{'' points,} \\
&D_x u^{n+1} + D_y v^{n+1} = 0, \\
&\quad \text{at ``}\square\text{'' points.}
\end{aligned} \tag{4.4}$$

Applying the discrete divergence operator on the momentum equations, we obtain an equation for p^n in the form

$$\Delta_h p^n = \text{terms involve } \mathbf{u}^n. \tag{4.5}$$

The boundary condition is already included in (4.5). We denote the solution of this equation by $p^n = \mathscr{F}(\mathbf{u}^n)$.

4.2. *The MAC Scheme and Thom's Formula*

Let us first examine the MAC scheme in the linear case and return to the mesh in Fig. 3. Define the discrete vorticity at ``●'' points as

$$\omega_{i,j} = (\nabla_h \times \mathbf{u})_{i,j} = -\frac{u_{i,j+1/2} - u_{i,j-1/2}}{\Delta y} + \frac{v_{i+1/2,j} - v_{i-1/2,j}}{\Delta x}. \tag{4.6}$$

Applying the discrete curl operator to (4.2) (dropping the nonlinear terms), we get

$$\frac{d\omega}{dt} = \nu \Delta_h \omega, \quad \text{at ``}\bullet\text{'' points.}$$

On Γ_x, we have

$$\omega_{i,0} = -\frac{2}{\Delta y} u_{i,1/2}. \tag{4.7}$$

On the other hand, if we define $\tilde{\psi}$ at the ``●'' points by

$$\tilde{\psi}_{i,0} = 0, \quad u_{i,j-1/2} = -\frac{\tilde{\psi}_{i,j} - \tilde{\psi}_{i,j-1}}{\Delta y}, \quad j \geq 1, \tag{4.8}$$

then from (4.2), we have

$$v_{i-1/2,j} = \frac{\tilde{\psi}_{i,j} - \tilde{\psi}_{i-1,j}}{\Delta x}, \quad \tilde{\psi}_{0,j} = 0, \tag{4.9}$$

and

$$\Delta_h \tilde{\psi} = \omega, \quad \text{at ``}\bullet\text{'' points.}$$

Therefore we have $\tilde{\psi} = \psi$. Going back to (4.6), we get

$$\omega_{i,0} = \frac{2}{\Delta y^2} \psi_{i,1}$$

which is Thom's formula. This shows that for the unsteady Stokes equation, the MAC scheme and Thom's formula, coupled with the standard centered difference for the stream function–vorticity formulation are the same method. The same is true for the fully discrete schemes.

There are other ways of treating the boundary for the MAC scheme. For convenience, we summarized these in Table I in Section 2 and listed the equivalent vorticity boundary conditions. In particular, we note that the improved formula of Peyret and Taylor [14, (6.2.20a)] corresponds to the first formula of Orszag and Israeli.

When the nonlinear terms are taken into account, (2.2) and (4.2) are not exactly the same any longer. They differ by a quantity of $O(\Delta x^2 + \Delta y^2)$. However, a tedious calculation shows that (4.2) is the same as

$$\begin{aligned}
&\frac{d\omega}{dt} - \frac{1}{2}[\tilde{D}_y \psi \tilde{D}_x \omega + \tilde{D}_x(\tilde{D}_y \psi\, \omega)] \\
&\quad + \frac{1}{2}[\tilde{D}_x \psi \tilde{D}_y \omega + \tilde{D}_y(\tilde{D}_x \psi\, \omega)] = \nu \Delta_h \omega, \\
&\Delta_h \psi = \omega,
\end{aligned} \tag{4.10}$$

at the ``●'' points. The details of that calculation is presented in Appendix 1. There is also an obvious analogous statement for the fully discrete schemes.

It is instructive to further explore this equivalence between vorticity-stream function and primitive variable formulations with the forward Euler replaced by the classical Runge–Kutta method. In the vorticity-stream function formulation the resulting method is the following: Given $\{\omega^n, \psi^n\}_{i,j\geq 0}$, compute $\{\omega^{n+1}, \psi^{n+1}\}_{i,j\geq 0}$ by

$$\frac{\omega_1 - \omega^n}{\frac{1}{2}\Delta t} + (\mathbf{u}^n \cdot \nabla_h)\omega^n = \nu \Delta_h \omega^n, \quad \psi_1 = \Delta_{h,0}^{-1}\omega_1,$$

$$\frac{\omega_2 - \omega^n}{\frac{1}{2}\Delta t} + (\mathbf{u}_1 \cdot \nabla_h)\omega_1 = \nu \Delta_h \omega_1, \quad \psi_2 = \Delta_{h,0}^{-1}\omega_2,$$

$$\frac{\omega_3 - \omega^n}{\Delta t} + (\mathbf{u}_2 \cdot \nabla_h)\omega_2 = \nu \Delta_h \omega_2, \quad \psi_3 = \Delta_{h,0}^{-1}\omega_3,$$

$$k_4 = -\Delta t((\mathbf{u}_3 \cdot \nabla_h)\omega_3 - \nu \Delta_h \omega_3)$$

$$\omega^{n+1} = \tfrac{1}{3}(-\omega^n + \omega_1 + 2\omega_2 + \omega_3) + \tfrac{1}{6}k_4, \quad \psi^{n+1} = \Delta_{h,0}^{-1}\omega^{n+1}$$

At every stage, the boundary value of vorticity is given by Thom's formula. The corresponding fully discrete MAC scheme is then

$$\frac{\mathbf{u}_1 - \mathbf{u}^n}{\frac{1}{2}\Delta t} + (\mathbf{u}^n \cdot \nabla_h)\mathbf{u}^n + \nabla_h p^n = \nu \Delta_h \mathbf{u}^n, \quad p_1 = \mathscr{F}(\mathbf{u}_1)$$

$$\frac{\mathbf{u}_2 - \mathbf{u}^n}{\frac{1}{2}\Delta t} + (\mathbf{u}_1 \cdot \nabla_h)\mathbf{u}_1 + \nabla_h p_1 = \nu \Delta_h \mathbf{u}_1, \quad p_2 = \mathscr{F}(\mathbf{u}_2)$$

$$\frac{\mathbf{u}_3 - \mathbf{u}^n}{\Delta t} + (\mathbf{u}_2 \cdot \nabla_h)\mathbf{u}_2 + \nabla_h p_2 = \nu \Delta_h \mathbf{u}_2, \quad p_3 = \mathscr{F}(\mathbf{u}_3)$$

$$k_4 = -\Delta t((\mathbf{u}_3 \cdot \nabla_h)\mathbf{u}_3 + \nabla_h p_3 - \nu \Delta_h \mathbf{u}_3)$$

$$\mathbf{u}^{n+1} = \tfrac{1}{3}(-\mathbf{u}^n + \mathbf{u}_1 + 2\mathbf{u}_2 + \mathbf{u}_3) + \tfrac{1}{6}k_4, \quad p^{n+1} = \mathscr{F}(\mathbf{u}^{n+1}).$$

Here we have written the nonlinear terms loosely as $(\mathbf{u} \cdot \nabla_h)\mathbf{u}$. The full expression should be the one in (4.2). Of course, for these two methods to be exactly the same, we have to use the more complicated discretization for the convection term as in (4.10).

This time-stepping procedure is very similar to the one proposed by Johansson [11].

To illustrate the efficiency of these methods and the importance of the high order Runge–Kutta procedure, we present some numerical results for a canonical problem: the driven cavity flow. The flow domain is $[0, 1] \times [0, 1]$. We impose the no-slip condition. The upper boundary moves with the velocity: $u_b(x) = 1$ or $16x^2(1 - x^2)$. The initial data is chosen to be: $\psi_0(x, y) = (y^2 - y^3)u_b(x)$.

First in Fig. 4 we show the numerical results for the case $u_b(x) = 1$ at Reynolds number 10^4, $t = 100$. This is a standard test problem. There is a vast amount of numerical work on this. Most of them, however, solve the steady state equation directly [6, 19]. Although the methods presented above should not be advertised for steady state calculations, they perform reasonably well for this problem. At $t = 100$, the flow has all the characteristic features of the steady state [6]. However, at this point it is not entirely clear whether the flow eventually reaches steady state in such an unsteady calculation.

In Figs. 5–8 we show our numerical results with the boundary condition $u_b(x) = 16x^2(1 - x^2)$ at Reynolds number 10^5. These were computed on a 1024^2 grid with viscosity $\nu = 10^{-5}$. We verified these numerical results using the fourth-order scheme designed in [4] on 512^2 and 1024^2 grids. Notice the extremely unsteady turbulent behavior as a result of the boundary layer separations.

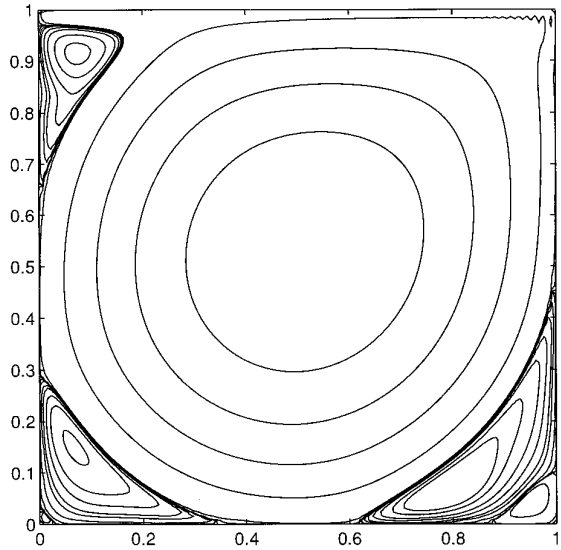

FIG. 4. Driven cavity flow with $u_b(x) = 1$ at Reynolds number 10^4, $t = 100$, computed with the explicit MAC scheme with fourth-order Runge–Kutta in time. Shown here is the contour plot of stream function. Parameters: viscosity = 10^{-4}, CFL = 1.25, $\Delta x = \frac{1}{128}$.

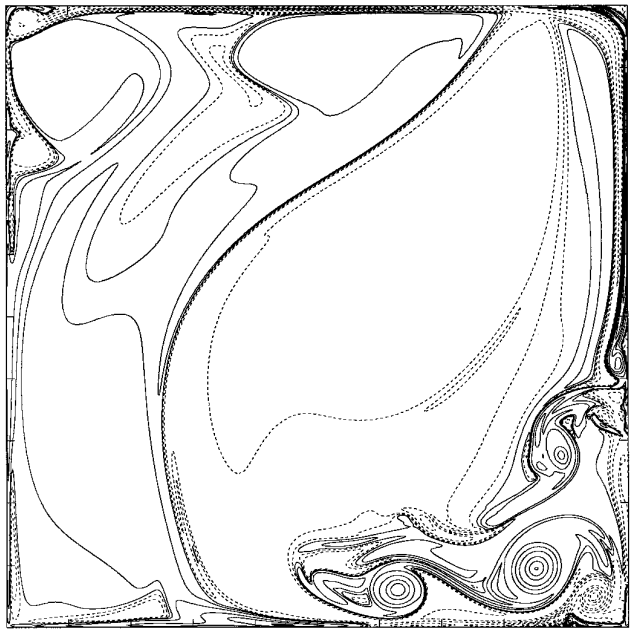

FIG. 5. The driven cavity problem at $t = 5$ and Reynolds number 10^5 computed using the explicit Thom's formula with fourth-order Runge–Kutta in time. Shown here is the contour plot of vorticity. Vortices are shed at the lower right corner as a result of the boundary layer separation. Parameters: viscosity = 10^{-5}, CFL = 1.25, $\Delta x = \frac{1}{1024}$.

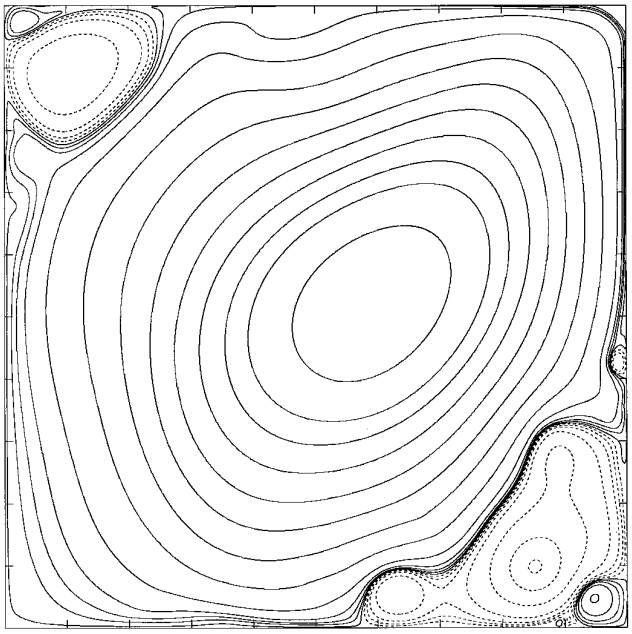

FIG. 6. Same as Fig. 5, but for the stream function. At the lower right and upper left corners, the primary vortex has induced two generations of secondary vortices.

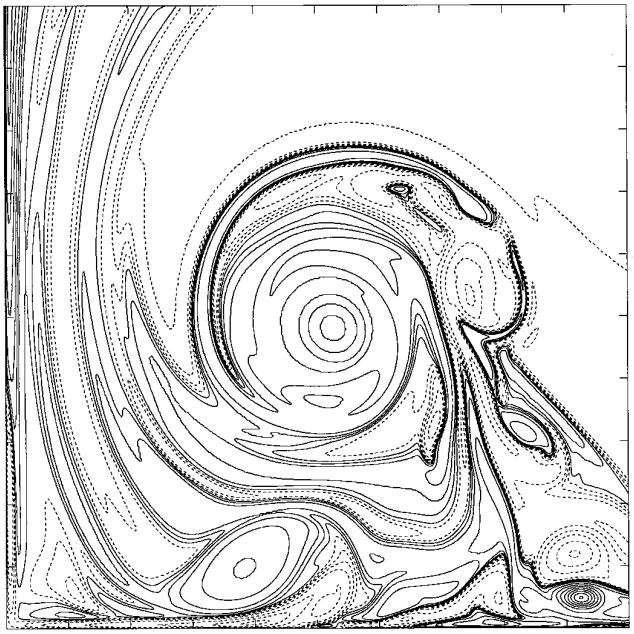

FIG. 7. The driven cavity problem at $t = 8$. Plotted here is the vorticity at the lower left quadrant. The contour lines are severely stretched. A mushroom-like structure forms as a result of the collision of vortices. Parameters: viscosity = 10^{-5}, CFL = 1.25, $\Delta x = \frac{1}{1024}$.

The calculation reported here took approximately 2 h on the C-90 machine with a single processor at the Pittsburgh Supercomputing Center. A similar calculation on a smaller mesh 512^2 with a smaller Reynolds number ($\nu = 3 \times 10^{-5}$) was done on a SPARC-10 work-station, and that took about three days. Obviously there is a lot of room for improvement. We will return to this in a separate paper [4].

5. CONCLUSIONS

Let us summarize the issues discussed in this paper.

The first issue we discussed was the local and global vorticity boundary conditions. We showed that Anderson's global vorticity boundary condition can always be realized by local formulas, the simplest case being Fromm's formula. The non-locality of Quartapelle's vorticity boundary condition comes from the fact that the viscous term is insisted to be treated implicitly. Therefore even the seemingly local vorticity boundary condition turns out to be global.

A majority of the discussions in the literature on global vorticity boundary conditions resemble Quartapelle's, so the global nature of the vorticity boundary condition is really a result of the implicit treatment of the viscous term.

The second issue we discussed is the cell Reynolds number constraint in connection with the fact that the convection terms are treated using centered differences. We explained that while there is a severe constraint on the cell Reynolds number given by stability when first- and second-order Runge–Kutta methods are used in time, such constraints disappear for higher order Runge–Kutta methods. This is a significant fact with regard to the efficiency of centered schemes.

The third issue we discussed is the relation between the MAC scheme and the second-order centered difference schemes in the vorticity-stream function formulation, coupled with various local formulas for the vorticity boundary condition. We showed that the MAC scheme is the same as the standard second-order centered difference scheme in the vorticity-stream function formulation, and the local formulas for the vorticity boundary condition can be translated into local formulas for the velocity boundary condition and vice versa. In particular, Thom's formula translates to the reflection boundary condition for the MAC scheme.

From these discussions we arrive at the following basic design principles: (1) The viscous term should be treated explicitly for finite difference schemes in the vorticity-stream function formulation. If one insists on treating the viscous terms implicitly, then it is much better to use the projection method [3]. (2) One should use at least third-order Runge–Kutta methods in time in connection with centered differences in space for high Reynolds number flows.

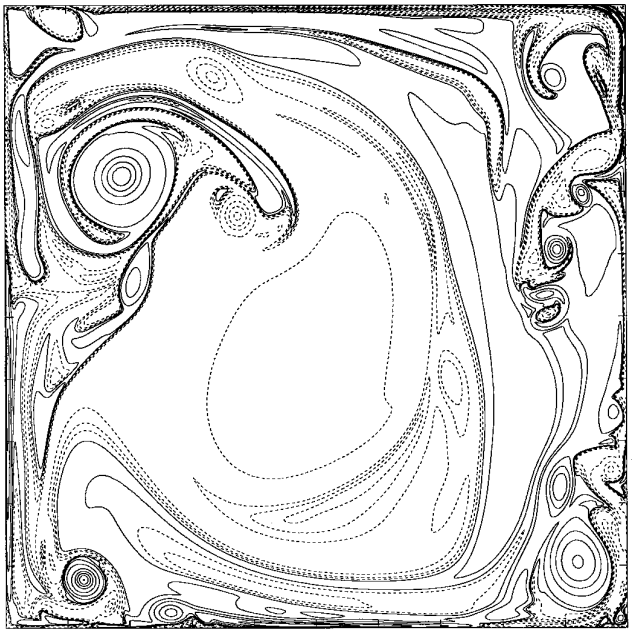

FIG. 8. The driven cavity problem at $t = 10$. The flow is now considerably more turbulent than in Figs. 5–6. A lot of small vortices form. Parameters: viscosity = 10^{-5}, CFL = 1.25, $\Delta x = \frac{1}{1024}$.

APPENDIX 1: NONLINEAR TERMS

Applying the discrete curl operator to (4.2), we get

$$\frac{d\omega}{dt} + N(u, v) = \nu \Delta_h \omega, \quad \text{at ``●'' points,}$$

where

$$\begin{aligned} N(u, v) = &-D_y(u\, D_x^0 u + E_x E_y v\, \mathrm{D}_y^0 u) \\ &+ D_x(E_x E_y u\, D_x^0 v + v\, D_y^0 v). \end{aligned}$$

Using

$$D_x(uv) = D_x u\, E_x v + E_x u\, D_x v,$$

we have

$$\begin{aligned} N(u, v) = &-E_y u \tilde{D}_x D_y u - E_x v \tilde{D}_y D_y u \\ &+ (I - E_y^2) E_x v \tilde{D}_y D_y u + E_y u \tilde{D}_x D_x v \\ &+ E_x v \tilde{D}_y D_x v + (E_x^2 - I) E_y u \tilde{D}_x D_x v \\ &- D_y u\, E_x E_y\, D_x u - E_x E_y\, D_y v\, E_y^2\, D_y u \\ &+ (I - E_y^2)\, D_y u\, E_x E_y\, D_y v + E_x E_y\, D_x u\, E_x^2\, D_x v \\ &+ D_x v\, E_x E_y\, D_y v + (E_x^2 - I)\, D_x v\, E_x E_y\, D_x u. \end{aligned}$$

Since

$$E_x^2 - I = \frac{h^2}{4} D_x^2, \quad E_y^2 - I = \frac{h^2}{4} D_y^2,$$

we get

$$\begin{aligned} N(u, v) = &E_y u\, \tilde{D}_x \omega + E_x v\, \tilde{D}_y \omega \\ &+ \frac{h^2}{4}(-D_y^2 E_x v \tilde{D}_y D_y u + D_x^2 E_y u \tilde{D}_x D_x v \\ &- D_y^2 D_y u\, E_x E_y\, D_y v + D_x^2 D_x v\, E_x E_y\, D_x u). \end{aligned}$$

From (4.6)–(4.7) and

$$\tilde{D}_x u = D_x E_x u$$

we have

$$\begin{aligned} N(u, v) = &-\tilde{D}_y \psi\, \tilde{D}_x \omega + \tilde{D}_x \psi\, \tilde{D}_y \omega \\ &+ \frac{h^2}{4}(D_y^2 \tilde{D}_x \psi\, \tilde{D}_y \tilde{D}_y^2 \psi - D_x^2 \tilde{D}_y \psi\, \tilde{D}_x D_x^2 \psi \\ &+ D_y^4 \psi\, \tilde{D}_x \tilde{D}_y \psi - D_x^4 \psi\, \tilde{D}_x \tilde{D}_y \psi). \end{aligned}$$

Direct computation gives us

$$\begin{aligned} N(u, v) = &-\tilde{D}_y \psi\, \tilde{D}_x \omega + \tilde{D}_x \psi\, \tilde{D}_y \omega \\ &+ \frac{h^2}{4}(D_y^2 \tilde{D}_x \psi\, \tilde{D}_y \Delta_h \psi - D_x^2 \tilde{D}_y \psi\, \tilde{D}_x \Delta_h \psi \\ &+ D_y^2 \Delta_h \psi\, \tilde{D}_x \tilde{D}_y \psi - D_x^2 \Delta_h \psi\, \tilde{D}_x \tilde{D}_y \psi) \\ = &-\tilde{D}_y \psi\, \tilde{D}_x \omega + \tilde{D}_x \psi\, \tilde{D}_y \omega \\ &+ \frac{h^2}{4}(D_y^2 \tilde{D}_x \psi\, \tilde{D}_y \omega - D_x^2 \tilde{D}_y \psi\, \tilde{D}_x \omega \\ &+ D_y^2 \omega\, \tilde{D}_x \tilde{D}_y \psi - D_x^2 \omega\, \tilde{D}_x \tilde{D}_y \psi). \end{aligned}$$

Similarly, using

$$\tilde{D}_x(uv) = \tilde{D}_x u\, \tilde{E}_x v + \tilde{E}_x u\, \tilde{D}_x v$$

$$\tilde{E}_x - I = \frac{h^2}{2} D_x^2, \quad \tilde{E}_y - I = \frac{h^2}{2} D_y^2,$$

we have

$$
\begin{aligned}
&-\tilde{D}_x(\tilde{D}_y\psi\,\omega) + \tilde{D}_y(\tilde{D}_x\psi\,\omega)\\
&\quad = -\tilde{D}_y\psi\,\tilde{D}_x\omega + \tilde{D}_x\psi\,\tilde{D}_y\omega + (I-\tilde{E}_x)\,\tilde{D}_y\psi\,\tilde{D}_x\omega\\
&\qquad + (\tilde{E}_y - I)\,\tilde{D}_x\psi\,\tilde{D}_y\omega + (I-\tilde{E}_x)\omega\,\tilde{D}_x\,\tilde{D}_y\psi\\
&\qquad + (\tilde{E}_y - I)\omega\,\tilde{D}_y\,\tilde{D}_x\psi\\
&\quad = -\tilde{D}_y\psi\,\tilde{D}_x\omega + \tilde{D}_x\psi\,\tilde{D}_y\omega\\
&\qquad + \frac{h^2}{2}(-D_x^2\,\tilde{D}_y\psi\,\tilde{D}_x\omega + D_y^2\,\tilde{D}_x\psi\,\tilde{D}_y\omega\\
&\qquad - D_x^2\omega\,\tilde{D}_x\,\tilde{D}_y\psi + D_y^2\omega\,\tilde{D}_y\,\tilde{D}_x\psi).
\end{aligned}
$$

Therefore,

$$
\begin{aligned}
N(u,v) &= -\tilde{D}_y\psi\,\tilde{D}_x\omega\\
&\quad + \tilde{D}_x\psi\,\tilde{D}_y\omega + \tfrac{1}{2}[\tilde{D}_y\psi\,\tilde{D}_x\omega - \tilde{D}_x(\tilde{D}_y\psi\,\omega)]\\
&\quad - \tfrac{1}{2}[\tilde{D}_x\psi\,\tilde{D}_y\omega - \tilde{D}_y(\tilde{D}_x\psi\,\omega)]\\
&= -\tfrac{1}{2}[\tilde{D}_y\psi\,\tilde{D}_x\omega + \tilde{D}_x(\tilde{D}_y\psi\,\omega)]\\
&\quad + \tfrac{1}{2}[\tilde{D}_x\psi\,\tilde{D}_y\omega + \tilde{D}_y(\tilde{D}_x\psi\,\omega)].
\end{aligned}
$$

APPENDIX 2: CONSISTENCY NEAR THE BOUNDARY FOR THE REFLECTION TECHNIQUE

If we use the reflection boundary condition $u_{i,-1/2} + u_{i,1/2} = 0$ in the MAC scheme, a simple truncation error analysis at $x_{1/2}$ gives

$$
D_x^2 u(x_{1/2} = \frac{3}{4}u''(x_{1/2}) + \frac{h}{8}u'''(0) + O(h^2),
$$

suggesting that the operator D_x^2 is not consistent with the Laplacian near the boundary. This issue has been raised in several places, including [14]. We show here that a more sophisticated error analysis reveals that the overall scheme still has second-order accuracy. We explain this by a simple example

$$
u'' = f, \quad u(0) = (1) = 0
$$

with the standard centered difference applied to the grid points $x_{i+1/2} = (i + \frac{1}{2})\,\Delta x$, $i = 0, 1, \ldots, n-1$ and the boundary condition $u_{-1/2} + u_{1/2} = 0$, $u_{n+1/2} + u_{n-1/2} = 0$. Let

$$
\bar{u}_{i+1/2} = u(x_{i+1/2}) - \frac{h^2}{8}[u''(0) + (u''(1) - u''(0))x_{i+1/2}]
$$

for $i = 0, 1, \ldots, n-1$

and

$$
\bar{u}_{-1/2} = -\bar{u}_{1/2}, \quad \bar{u}_{n+1/2} = -\bar{u}_{n-1/2}.
$$

Clearly,

$$
D_x^2\bar{u}_{i+1/2} = u''(x_{i+1/2}) + O(h^2) \quad \text{for } i = 1, \ldots, n-2.
$$

At $x_{1/2}$,

$$
\begin{aligned}
D_x^2\bar{u}_{1/2} &= \frac{\bar{u}_{3/2} - 3\bar{u}_{3/2}}{h^2} = \frac{u(x_{3/2}) - 3u(x_{3/2})}{h^2} + \frac{1}{4}u''(0)\\
&= \frac{3}{4}u''(x_{1/2}) + \frac{h}{8}u'''(0) - \frac{1}{4}u''(0) + O(h^2)\\
&= u''(x_{1/2}) + O(h^2).
\end{aligned}
$$

Similarly, we have

$$
\begin{aligned}
D_x^2\bar{u}_{n-1/2} &= \frac{u(x_{n-3/2}) - 3u(x_{n-3/2})}{h^2} + \frac{1}{4}u''(1)\\
&= u''(x_{n-1/2}) + O(h^2).
\end{aligned}
$$

This gives

$$
u(x_{i+1/2}) - u_{i+1/2} = O(h^2).
$$

The boundary condition mentioned in [14],

$$
u_{-1/2} = \tfrac{1}{3}(u_{3/2} - 6u_{1/2} + 8u_\Gamma),
$$

corresponds to the first formula of Orszag and Israeli (see Table I in Section 2).

ACKNOWLEDGMENTS

We are very grateful to Gretar Tryggvason for his suggestions which greatly improved the presentation of this paper. We also thank Alexander Chorin for very helpful discussions. The work of Weinan E was supported by the NEC Research Institute Inc., the Sloan Foundation under Grant 93-6-6, a Sloan Foundation Fellowship, and NSF Grant DMS-9303779. The work of J.-G. Liu was supported in part by NSF Grants DMS-9505275 and DMS-9304580. The computations were done at the Pittsburgh Supercomputing Center.

REFERENCES

1. C. R. Anderson, *J. Comput. Phys.* **80,** 72 (1989).
2. W. R. Briley, *J. Fluid Mech.* **47,** 713 (1971).
3. A. J. Chorin, *Math. Comput.* **22,** 745 (1968).
4. W. E and J.-G. Liu, *J. Comput. Phys.,* submitted.
5. W. E and J.-G. Liu, preprint.
6. U. Ghia, K. N. Ghia, and C. T. Shin, *J. Comput. Phys.* **48,** 387 (1982).
7. P. M. Gresho, *Annu. Rev. Fluid Mech.* **23,** 413 (1991).
8. P. M. Gresho, *Adv. Appl. Mech.* **28,** 45 (1992).
9. F. H. Harlow and J. E. Welch, *Phys. Fluids* **8,** 2182 (1965).

10. H. D. Henshaw, H.-O. Kreiss, and L. G. M. Reyna, *Comput. & Fluids,* to appear.
11. B. C. Johansson, *J. Comput. Phys.* **105,** 233 (1993).
12. S. A. Orszag and M. Israeli, *Annu. Rev. Fluid Mech.* **6,** 281 (1974).
13. S. A. Orszag, M. Israeli, and M. O. Deville, *J. Sci. Comput.* **1,** 75 (1986).
14. R. Peyret and T. Taylor, *Computational Methods for Fluid Flow* (Springer-Verlag, New York/Berlin, 1983).
15. L. Quartapelle, *Numerical Solution of the Incompressible Navier–Stokes Equations* (Birkhäuser, Berlin, 1983).
16. L. Quartapelle and F. Valz-Gris, *Int. J. Numer. Methods Fluids* **1,** 129 (1993).
17. M. Reider, Ph.D. dissertation, UCLA, 1992 (unpublished).
18. P. J. Roache, *Computational Fluid Dynamics* (Hermosa, Albuquerque, NM, 1982).
19. R. Schreiber and H. B. Keller, *J. Comput. Phys.* **49,** 310 (1983).
20. A. Thom, *Proc. Roy. Soc. London Sect. A* **141,** 651 (1933).
21. D. C. Thoman and A. A. Szewczyk, *Phys. Fluids* **12** (1969), II-76–II-87.